Solar Energy 157 (2017) 707–712

Contents lists available at ScienceDirect

Solar Energy

journal homepage: www.elsevier.com/locate/solener

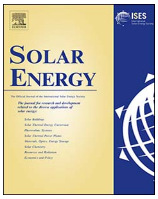

An approach to ZnTe:O intermediate-band photovoltaic materials

Nan Tang[a], Qimin Hu[a], Aobo Ren[a], Wei Li[a,*], Cai Liu[a,*], Jingquan Zhang[a], Lili Wu[a], Bing Li[a], Guanggen Zeng[a], Songbai Hu[b]

[a] College of Materials Science and Engineering, Sichuan University, Chengdu 610064, China
[b] Department of Physics, South University of Science and Technology, Shenzhen 518055, China

ARTICLE INFO

Keywords:
Intermediate band
ZnTe:O
Molecular beam epitaxy
Ion implantation

ABSTRACT

ZnTe epitaxial layers with different crystalline quality were grown by molecular beam epitaxy. ZnTe:O was achieved by oxygen incorporation in ZnTe films using ion implantation. The proper concentrations of O ions attributed to the formation of the intermediate band which was approximately 1.88 eV above the valence band maximum. Pulsed laser melting was then carried out on the samples. ZnTe with high crystalline quality and appropriate concentrations of oxygen ions led to the improvements of absorption efficiency of the intermediate band. The results suggest that factors such as the crystalline quality and the dose of O concentration are important to achieve better ZnTe:O intermediate-band photovoltaic materials. The way we utilize to fabricate ZnTe:O intermediate band solar cell materials is applicable, and the position and intensity of O states could be well controlled.

1. Introduction

Intermediate band solar cell (IBSC) is one of the third generation solar cells with high power conversion efficiency, low cost and simple structure, which is promising and attractive (Okada et al., 2015; Ramiro et al., 2014; Wang et al., 2011a, 2009; Kim et al., 2014; Lv et al., 2014; Razykov et al., 2011; Luque et al., 2005). With the existence of an energy level in the band-gap, the intermediate band (IB) is possible to collect more photons which are wasted in the conventional single gap solar cells. The photon absorption process occurs as follows: low energy photons pump electrons from the valence band (VB) to the IB and from the IB to the conduction band (CB). In this way, two below-bandgap energy photons create one net electron-hole pair that adds to the ones generated conventionally through transitions from the VB to the CB. Quantum dots and highly mismatched alloys (HMAs) may be two important ways to obtain IBSCs. Contrast to the quantum dots with discrete energy levels of confined states produced in the host material by the internal film strain which limits the cell efficiency and affects the material structure (Ramiro et al., 2014; Wang et al., 2011a; Kim et al., 2014; Gorji, 2012), the IB obtained by the HMAs is not difficult to fabricate. Dilute oxygen doped ZnTe as the absorber has been one of the prototypes of HMAs to demonstrate the concept of IBSC sufficiently, e.g., $n^{\pm}$-ZnO/i-ZnTeO/p-ZnTe (Okada et al., 2015), $n^{\pm}$-GaAs/p-ZnTeO/$p^{\pm}$-ZnTe (Wang et al., 2011a, 2009). The traditional method to achieve ZnTe:O intermediate band is either by using RF-plasma assisted molecular beam epitaxy (MBE) called for *in-situ* doping, or single crystal ZnTe wafer doped with oxygen by ion implantation called for *ex-situ* doping. For the latter, it is not suitable for the further industrial fabrication and far more expensive due to the high price of bulk ZnTe wafer, but the depth and concentration of doping can be precisely controlled (Antolín et al., 2014; Ye et al., 2014). For the former, it is a one-step method for facile fabrication of oxygen incorporated ZnTe thin films, however, the *in-situ* doping for ZnTe:O intermediate band cannot solve the problems of the position of Fermi level and the solubility limitation.

In this work, combined with the merits of two classical methods, a new approach to acquire ZnTe:O materials has been proposed in order to solve the problems of *in-situ* doping and *ex-situ* doping as mentioned above. ZnTe:O materials are achieved by ion implantation, after the ZnTe growth on GaAs substrate in MBE chamber. In this way, the depth and dose of oxygen can be better controlled than that of *in-situ* doping. Also, the device can be readily fabricated and costs less compared with bulk ZnTe doped with oxygen. As we know, ion implantation causes damage in the near-surface region of ZnTe and not all of the implanted impurities occupy regular lattice sites. ZnTe:O was then annealed by pulsed laser melting (PLM) to recover the crystal quality, thus allowing for a higher solute trapping of O in the Te lattice (Yang et al., 2014; García-Hemme et al., 2013; Galenko et al., 2011; White et al., 1980). During this process, the IB to CB transition can be significantly improved.

---

* Corresponding authors.
E-mail address: waylee2000@sohu.com (W. Li).

http://dx.doi.org/10.1016/j.solener.2017.08.078
Received 21 June 2017; Received in revised form 27 August 2017; Accepted 29 August 2017

2. Experimental details

ZnTe host materials were grown by the MBE system using solid Zn (6N) and Te (6N) as source materials on 2-inch GaAs (1 0 0) substrates. GaAs was put in the pretreatment chamber for 3 h thermal treatment at 480 °C and the growth chamber for 30 min deoxidization at 680 °C before ZnTe epilayer growth. The optimal substrate temperature was controlled at 330 °C while growing. Zn source was opened for 10 s before ZnTe growing, for avoiding the formation of Ga–Te bonds which was not beneficial for ZnTe epilayer growth, and then the Te shutter was opened. We maintained the source temperatures of Zn for samples at 260 °C, while Te temperatures for each of ZnTe series were varied, where 1# was 290 °C, 2# was 300 °C, and 3# was 310 °C. Due to the high melting temperature of Te in high vacuum, temperature of Te under 290 °C was difficult to achieve the stoichiometric ZnTe thin films when fixing Zn source at 260 °C. The total time of ZnTe growth was about 60–90 min. So, three series of ZnTe with different crystalline quality were prepared. After that, ion implantation and PLM processes were performed on the samples because fabrication techniques under the thermodynamic equilibrium would not be suitable to get over the difficulty of the solid solubility limit. First, it was the doping progress by ion implantation and with which angle of reflection between O ions and samples was about 70°, O ions were incorporated into ZnTe. In order to obtain the doping profile of O ions in ZnTe epilayers, it was necessary to use the stopping and range of ions in matter (SRIM) of Monte Carlo methods to simulate the ion stopping and ion range distribution after implantation (Suzuki et al., 2009; Hane et al., 1997). Therefore the ion implantation dose and target depth were much more controllable and accurate than common doping method by vacuum evaporation. The redistribution of oxygen after ion implantation was confirmed using secondary ion mass spectrometry (SIMS). Nevertheless, ion incorporation causes damage in the near-surface region of semiconductors and may even results in the implanted impurities generally not occupy regular lattice sites and are not electrically active. The high-power density radiation from pulsed laser is commonly used to anneal ion-implanted semiconductors, which can lead to rapid melting and recrystallization of semiconductors several thousand angstroms thick (Galenko et al., 2011; White et al., 1980). In this work, all the ZnTe:O samples were taken to anneal in air by a pulsed KrF excimer laser (wavelength 248 nm) at an energy density of 0.4 J/cm^2 and a pulse duration time of 20 ns. The area annealed on each sample was about 1 cm^2. The PLM conditions were sufficient to cause the melt front to penetrate the damage region into the GaAs crystal bulk on which epitaxial regrowth could occur rather than sublimation of the thin films. X-ray diffraction (XRD) measurements were used to analyze the structural properties of samples and the quality of crystal thin films such as the full width at half maximum (FWHM) and reciprocal space maps (RSMs). The surface morphology and thickness of samples were investigated by scanning electron microscope (SEM). Transmission electron microscope (TEM) samples were prepared with cross-sectional geometry (Wang et al., 2011b), in which two small pieces of the sample were glued together with adjoining ZnTe surfaces, and then polished to thickness of less than 20 um, finally two edges of it was thinned with argon-ion milling to about 100 nm. The high-resolution images of cross section for the specimen were characterized using a high-resolution transmission electron microscope (HRTEM). Selected-area electron diffraction (SAED) patterns were used to determine the orientation of samples. Room-temperature photoluminescence (PL) spectra obtained with a 425-nm-wavelength laser was used to characterize the optical properties.

3. Results and discussion

SRIM of Monte Carlo methods was used to simulate the ion stopping and ion range distribution after ion implantation. From Fig. 1(a), by controlling the total doses of O ions to be identical, O ion distribution varies with different ion energies. The depth of implantation becomes deeper as energy increases, and when implantation energy is 69 keV, the magnitude of peak of the depth is more than 100 nm contrasting to which, by using 15 keV, is less than 50 nm. However, the peak of O ion distribution becomes smaller as implantation energy increases. Fig. 1(b) shows multiple energies, 15, 40, and 69 keV, and different doses of O implantation are combined reasonably, which are then carried out on ZnTe samples grown by MBE, and it forms ZnTe:O with almost constant concentrations of oxygen incorporation for each of ZnTe series. The relationship between O ion concentration and dose is shown in Table 1 and we can achieve different O concentrations of 8.0×10^{20}, 4.0×10^{21} and 4.0×10^{22} cm^{-3} at about 150 nm for ZnTe films. To obtain the real oxygen migration in the ZnTe after ion implantation, the distribution was measured using SIMS. The two curves as shown in Fig. 1(b) have the same trend for O concentration from the depth of 25 to 350 nm at the O concentration of the order of 10^{21} cm^{-3}, demonstrating that ion implantation is controllable even when samples are doped by a large amount of ions. However, it shows some differences when the depth is less than 25 nm. This may be caused by the adsorption of O_2 in the air at the surface of the films, which makes the O concentration of SIMS a little higher than SRIM. Since the oxygen ions doped to ZnTe single crystal films with high energy would lead to the displacement of the lattice atoms, accompanying with the presence of some vacancy or interstitial defects, the oxygen ions are more likely to substitute the Te positions forming the IB. The vacancy damage distribution is shown in Fig. 1(c) from SRIM. By using 15, 40, and 69 keV as implantation energy, the total vacancy damage distribution almost decreases from 0 to 150 nm. It is worth noting that the O concentration quantified turns to become larger in the range 0–25 nm after PLM treatments from the SIMS results. This is due to a push out effect, which makes the O moves towards the surface as shown in Fig. 1(b) (Eric García-Hemme et al., 2013).

Fig. 2(a)–(c) shows XRD patterns of ZnTe for samples 1#, 2# and 3#, respectively. From Fig. 2(a), (2 0 0) and (4 0 0) peaks from ZnTe and (4 0 0) from GaAs substrate for 1# can be observed, demonstrating the formation of single crystalline epitaxial layer. Fig. 2(b) shows 2#, almost (1 0 0) orientation of ZnTe which consists of (2 0 0) and (4 0 0) reflection peaks. GaAs (2 0 0) and GaAs (4 0 0) are also seen, and the ZnTe thin films could be considered as single crystalline films. The FWHMs for samples1# and 2# are also shown in Fig. 2(a) and (b). The FWHM for 1# is 0.394°, much smaller than 2# of 2.138°, which means that 1# has much better crystalline quality than 2#. ZnTe (1 1 1) appears besides GaAs (2 0 0), GaAs (4 0 0) and ZnTe (2 0 0) for 3# whose source temperature for Te is 310 °C in Fig. 2(c), implying the polycrystalline nature with the (1 0 0) highly preferred-orientation ZnTe thin films. The morphology of cross section and surface for the sample is shown in Fig. 3 further supporting characteristics of worse arrangements for ZnTe with the existence of crystalline column. Fig. 2(d)–(f) shows XRD patterns for 1# as-grown, doped with O ions before and after PLM treatments. Due to the rapid cooling and epitaxial growth after reaching ZnTe melting temperature (White et al., 1979), the intensity of ZnTe (2 0 0) after PLM treatments, compared with that of ZnTe (2 0 0) before rapid thermal processing, has been significantly enhanced. However, the intensity of these ZnTe (2 0 0) samples is much weaker than that of as-deposited ZnTe thin films, demonstrating that the damage of ZnTe thin films is unavoidable after doping and the PLM treatment is effective to repair crystal quality. These results are also confirmed by FWHM of ZnTe (2 0 0). The FWHMs of ZnTe(2 0 0) for 1# as-deposited, doped with O ($\sim 4.0 \times 10^{21}$ cm^{-3}) before and after PLM treatments are 0.394°, 0.815° and 0.557°, respectively. Since the FWHM of 1# is much smaller than the other two, it means the worsening of the ZnTe quality. However, the FWHM of oxygen-incorporated ZnTe changes from 0.815° to 0.557° because of PLM treatments, which illustrates the enhancements of the crystal quality.

RSMs in the vicinity of the asymmetric (2 2 4) reflection were scanned using triple axis X-ray diffraction to evaluate stress relaxation